Available online at www.sciencedirect.com
ScienceDirect
Journal of Sound and Vibration 317 (2008) 308–328
JOURNAL OF SOUND AND VIBRATION
www.elsevier.com/locate/jsvi

Dynamics of a rectangular plate resting on an elastic foundation and partially in contact with a quiescent fluid

B. Uğurlu[a], A. Kutlu[b], A. Ergin[a,*], M.H. Omurtag[b]

[a]*Faculty of Naval Architecture and Ocean Engineering, Istanbul Technical University, Maslak 34469, Istanbul, Turkey*
[b]*Faculty of Civil Engineering, Istanbul Technical University, Maslak 34469, Istanbul, Turkey*

Received 9 March 2007; received in revised form 15 February 2008; accepted 10 March 2008
Handling Editor: A.V. Metrikine
Available online 8 May 2008

Abstract

In this study, a method of analysis is presented for investigating the effects of elastic foundation and fluid on the dynamic response characteristics (natural frequencies and associated mode shapes) of rectangular Kirchhoff plates. For the interaction of the Kirchhoff plate–Pasternak foundation, a mixed-type finite element formulation is employed by using the Gâteaux differential. The plate finite element adopted in this study is quadrilateral and isoparametric having four corner nodes, and at each node four degrees of freedom are present (one transverse displacement, two bending moments and one torsional moment). Therefore, a total number of 16 degrees-of-freedom are assigned to each element. A consistent mass formulation is used for the eigenvalue solution in the mixed finite element analysis. The plate structure considered is assumed clamped or simply supported along its edges and resting on a Pasternak foundation. Furthermore, the plate is fully or partially in contact with fresh water on its one side. For the calculation of the fluid–structure interaction effects (generalized fluid–structure interaction forces), a boundary element method is adopted together with the method of images in order to impose an appropriate boundary condition on the fluid's free surface. It is assumed that the fluid is ideal, i.e., inviscid, incompressible, and its motion is irrotational. It is also assumed that the plate–elastic foundation system vibrates in its *in vacuo* eigenmodes when it is in contact with fluid, and that each mode gives rise to a corresponding surface pressure distribution on the wetted surface of the structure. At the fluid–structure interface, continuity considerations require that the normal velocity of the fluid is equal to that of the structure. The normal velocities on the wetted surface of the structure are expressed in terms of the modal structural displacements, obtained from the finite element analysis. By using the boundary integral equation method the fluid pressure is eliminated from the problem, and the fluid–structure interaction forces are calculated in terms of the generalized hydrodynamic added mass coefficients (due to the inertial effect of fluid). To asses the influences of the elastic foundation and fluid on the dynamic behavior of the plate structure, the natural frequencies and associated mode shapes are presented. Furthermore, the influence of the submerging depth on the dynamic behavior is also investigated.

*Corresponding author. Tel.: +90 212 2856414; fax: +90 212 2856454.
E-mail address: ergina@itu.edu.tr (A. Ergin).

0022-460X/$ - see front matter © 2008 Elsevier Ltd. All rights reserved.
doi:10.1016/j.jsv.2008.03.022

1. Introduction

Plate structures have been widely used in various engineering fields, and their dynamic response behaviors are well studied and, therefore, a large number of publications can be found in the open literature (see, for instance, [1,2]). However, when they are resting on an elastic foundation and/or are partially or fully in contact with a fluid of comparable density, such as water, the foundation–structure and/or fluid–structure interaction effects play significant roles in their response behaviors and alter the dynamic states of the structures from those vibrating in the absence of fluid and foundation. Hence, the vibration behavior of the plate structures on elastic foundation and/or in contact with fluid is of great importance in structural, aerospace, civil, mechanical and marine engineering applications.

For the response behavior of elastic structures resting on an elastic foundation, a mechanical model is required to predict the interaction effects between the structure and foundation. Various mechanical models such as Winkler, Pasternak and Vlasov have been proposed in the open literature. The simplest mechanical model was developed by Winkler [3], which is generally referred to as a one-parametric model. The transverse deformation characteristics of the elastic foundation are defined by means of continuous and closely spaced linear springs. For instance, Gupta et al. [4] investigated the buckling and vibrational behavior of polar orthotropic circular plates resting on a Winkler-type foundation. The frequency values were calculated by using the Ritz method. It was observed that the presence of an elastic foundation increases the frequency values.

The deficiency of the Winkler formulation is the behavioral inconsistency due to the discontinuity of displacements on the boundary of the uniformly loaded surface area, and, therefore, two-parameter models were introduced. Among these models, the Pasternak formulation is the most popular one due to its simplicity. The second parameter in this model serves to represent the shear interaction between the plate and foundation. A number of pioneering finite element studies on static, dynamic and stability analysis of the Kirchhoff plate-Pasternak foundation interaction problems were conducted by Omurtag et al. [5], Özçelikörs et al. [6] and Doğruoğlu and Omurtag [7]. The free vibration results of Omurtag et al. [5] were also confirmed by the three-dimensional analysis of Zhou et al. [8]. Zhou et al. [8] determined the three-dimensional vibration characteristics of thick rectangular plates resting on an elastic foundation using the Pasternak model. Their analysis is based on the three-dimensional, small-strain, linear and exact elasticity theory, and the Ritz method was used to derive the frequency equation of the plate–foundation system by augmenting the strain energy of the plate with the elastic potential energy of the foundation. Eratlı and Aköz [9] solved the free vibration problem of a Reissner plate on a Pasternak foundation. Dumir [10] studied the von-Kármán-type, geometrically nonlinear, axisymmetric, static and transient responses of circular plates resting on a Pasternak foundation by using the point-collocation method for the spatial discretization, and the step-increment method for time. Shen et al. [11] investigated the free and forced vibration of the Reissner–Midlin plates with four free edges and resting on a Pasternak foundation by including the thermal effects. For the solution, they adopted the Rayleigh–Ritz method in conjunction with a set of admissible functions for satisfying both the geometrical and the natural boundary conditions. On the other hand, Xiang et al. [12] derived the analytical vibration and buckling solutions for simply supported, rectangular Mindlin plates on a Pasternak foundation. Wang et al. [13] obtained the relationship between the natural frequencies of the Reddy and Kirchhoff plates, with simply supported edge conditions. They also investigated the effects of initial stresses and Winkler–Pasternak foundation on the relationship. Very recently, Yu et al. [14] studied the dynamic responses of the Reissner–Mindlin plates resting on Winkler- and Pasternak-type elastic foundations. The formulations are based on the Reissner–Mindlin first-order shear deformation plate theory and including the plate–foundation interaction and thermal effects.

The fluid–structure interaction problems of plate structures partially or totally immersed in fluid have also received much attention due to their importance in various engineering fields. For instance, Ergin and Uğurlu [15] and Fu and Price [16] investigated the dynamic response characteristics (*wet* natural frequencies and associated mode shapes) of cantilever rectangular plates partially submerged in fluid. They observed that the frequency values of the plate structures decrease with increasing area of contact with fluid. Jeong et al. [17] studied the *wet* resonance frequencies and associated mode shapes of two identical rectangular plates coupled with a bounded fluid. The analytical method was developed by using a finite Fourier series expansion.

The frequencies of the in-phase vibrational modes of the plate structures were predicted well, but those of the out-of-phase vibrational modes could not be estimated precisely. On the other hand, Chang and Liu [18] calculated the natural frequencies of a rectangular isotropic plate in contact with fluid, for various boundary conditions. They observed that the *wet* modes were almost identical to the *dry* mode shapes. Meanwhile, the free vibration of circular plates in contact with fluid has been studied by various researchers (see, for instance, [19–21]).

Although a considerable amount of work dealing with the vibration of plate structures either resting on a foundation or in contact with fluid has been found in the open literature, few have been reported on the vibration of plates resting on an elastic foundation, and at the same time, in contact with fluid. Therefore, in this study, a method of analysis is presented for investigating the effects of an elastic foundation and fluid on the dynamic response characteristics (natural frequencies and associated mode shapes) of rectangular Kirchhoff plates. A mixed-type finite element formulation is employed, by using the Gâteaux differential for the derivation of the functional for the Kirchhoff plate–Pasternak-type elastic foundation interaction. The plate finite element PLTVE4 [5] is adopted in this study. It is a rectangular isoparametric-conforming C^0 class element having four corner nodes, and at each node four degrees of freedom are present (one transverse displacement, two bending moments and one torsional moment). Therefore, a total number of 16 degrees of freedom are assigned to each element. Since the functional does not have derivatives higher than first order, bilinear shape functions are used. The plate structure considered in this study is assumed to be clamped or simply supported along its edges and resting on a Pasternak foundation, and it is fully or partially in contact with fresh water, as illustrated in Fig. 1. By a Pasternak-type elastic foundation modeling, the influence of shear between the plate and foundation is inserted into the formulation by a shear layer besides the vertical spring elements (see Fig. 2).

In this paper, for the calculation of the fluid–structure interaction effects, a boundary element method is adopted together with the method of images, in order to impose an appropriate boundary condition on the fluid's free surface. The boundary element method presented in this study is already successfully applied to structures partially filled or partially submerged in a quiescent fluid (see, for example, Refs. [22,23]). However, the method is employed for a fluid–structure–foundation interaction problem (a rectangular plate structure in contact with an elastic foundation on its one side, and partially or fully in contact with fluid on the other side) for the first time (see Fig. 1). In this investigation, it is assumed that the fluid is ideal, i.e., inviscid, incompressible and its motion is irrotational. It is also assumed that the plate structure resting on the elastic

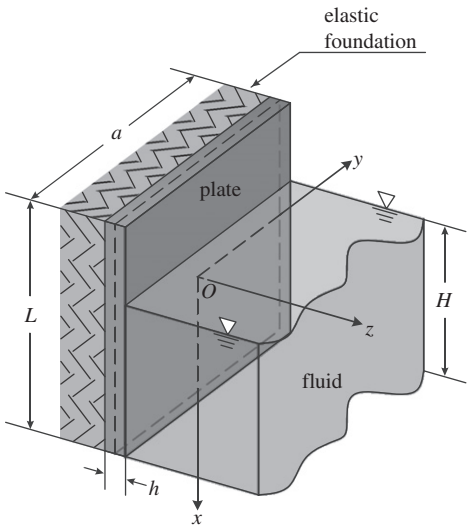

Fig. 1. Plate structure resting on a foundation and partially in contact with fluid.

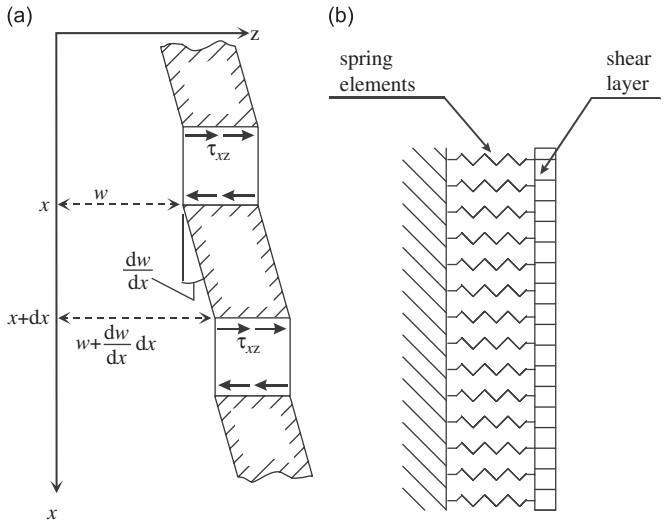

Fig. 2. Pasternak foundation: (a) shear layer element; (b) mechanical model.

foundation vibrates in its *in vacuo* eigenmodes when it is in contact with fluid, and that each mode gives rise to a corresponding surface pressure distribution on the wetted surface of the structure. The *in vacuo* dynamic analysis entails the vibration of the elastic plate–foundation system in the absence of any external force and structural damping, and the corresponding dynamic characteristics (e.g., natural frequencies and mode shapes) of the system were obtained by using a mixed-type finite element formulation and the plate finite element PLTVE4.

At the fluid–structure interface, continuity considerations require that the normal velocity of the fluid is equal to that of the structure. The normal velocities on the wetted surface of the structure are expressed in terms of the modal structural displacements, obtained from the finite element analysis of the plate–foundation system. By using a boundary integral equation method the fluid pressure is eliminated from the problem, and the fluid–structure interaction forces are calculated in terms of the generalized hydrodynamic added mass coefficients (due to the inertial effect of fluid).

In this analysis, the wetted surface is idealized by using appropriate boundary elements, referred to as hydrodynamic panels. The generalized structural mass matrix is merged with the generalized hydrodynamic added mass matrix. Then, the total generalized added mass and stiffness matrices are used together in solving the eigenvalue problem for the fluid–elastic plate–elastic foundation interaction problem. To asses the influence of the elastic foundation and fluid on the dynamic behavior of the plate structure, the natural frequencies and associated mode shapes are presented. Furthermore, the influence of the submerging depth ratio and various foundation types on the dynamic behavior of the plate structure is also investigated.

2. Mathematical model

2.1. Functional and mixed finite element formulation for foundation–plate interaction

2.1.1. Variational formulation

Before presenting the necessary steps for the mixed-type formulation based on the Gâteaux differential, some principal variational definitions are given. $\mathbf{Q}$ is a potential operator (positive definite and self-adjoint), if the equality $\langle d\mathbf{Q}(\mathbf{y};\bar{\mathbf{y}}),\mathbf{y}^*\rangle = \langle d\mathbf{Q}(\mathbf{y};\mathbf{y}^*),\bar{\mathbf{y}}\rangle$ is satisfied, where $d\mathbf{Q}(\mathbf{y};\bar{\mathbf{y}})$ and $d\mathbf{Q}(\mathbf{y};\mathbf{y}^*)$ are the Gâteaux derivatives of the operator in $\bar{\mathbf{y}}$ and $\mathbf{y}^*$ directions, respectively [24]. $\bar{\mathbf{y}}$ and $\mathbf{y}^*$ are field variables in different directions. Field equations can be written in an operator form as, $\mathbf{Q} = \mathbf{L}\mathbf{y} - \mathbf{f}$, where $\mathbf{L}$ is a differential

operator, **y** is the field variable vector and **f** is the load vector. If the operator **Q** is potential the corresponding functional for the field equations is obtained as follows:

$$I(y) = \int_0^1 [\mathbf{Q}(s\mathbf{y}; \mathbf{y}), \mathbf{y}]\mathrm{d}s, \tag{1}$$

where s is a scalar quantity.

2.1.2. Elastic foundation

The Pasternak model [25] is the most natural extension of the Winkler model [3], and it considers a shear interaction between the spring elements by connecting the ends of the springs to a plate of an incompressible shear layer (see Figs. 2 (a) and (b)), which deforms only due to transverse shears V_x and V_y:

$$V_x = \bar{G}\frac{\partial w}{\partial x} \quad \text{and} \quad V_y = \bar{G}\frac{\partial w}{\partial y}, \tag{2}$$

where $\bar{G}$ is the shear modulus of the foundation continuum and w represents the deflection of the shear layer. The coordinates x, y and z are shown in Fig. 3.

Recalling the lateral equilibrium in Fig. 3, the reaction–deflection relation of the shear layer and spring elements is given by

$$p_z = kw - \bar{G}\frac{\partial^2 w}{\partial x^2} - \bar{G}\frac{\partial^2 w}{\partial y^2}, \tag{3}$$

where p_z is the intensity of the reaction force of the foundation. The first parameter k is the modulus of the subgrade reaction of foundation. The last two terms on the right-hand side of equality (3) corresponds to the shear interaction of the shear layer. As a special case, if we let $\bar{G} = 0$, the above equation directly converges to a Winkler model.

2.1.3. Plate–foundation coupling

The positive directions of the coordinate axes (x,y,z), deflection w, bending moments K, M and torsional moment T are depicted in Fig. 3. Considering the plate–foundation interaction, the complete

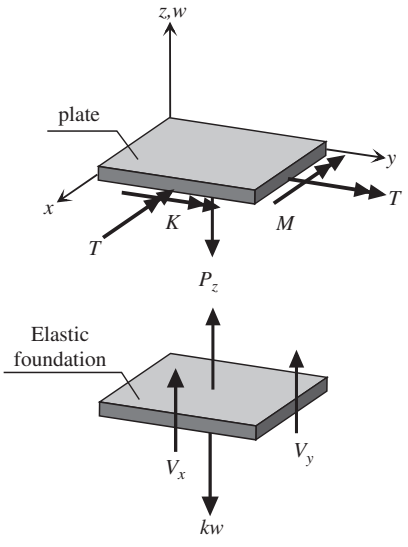

Fig. 3. Plate–elastic foundation interaction and positive directions of plates degrees of freedom.

set of field equations becomes

$$\left.\begin{aligned} -\frac{\partial^2 K}{\partial x^2}-\frac{\partial^2 M}{\partial y^2}-2\frac{\partial^2 T}{\partial x\,\partial y}+kw-\bar{G}\left(\frac{\partial^2 w}{\partial x^2}+\frac{\partial^2 w}{\partial y^2}\right)-\rho\frac{\partial^2 w}{\partial t^2}=0\\ -\frac{\partial^2 w}{\partial x^2}-\frac{12}{Eh^3}(K-\upsilon M)=0\\ -\frac{\partial^2 w}{\partial y^2}-\frac{12}{Eh^3}(M-\upsilon K)=0\\ -2\frac{\partial^2 w}{\partial x\,\partial y}-2(1+\upsilon)\frac{12}{Eh^3}T=0 \end{aligned}\right\}, \tag{4}$$

where E is the Young's modulus and υ is Poisson's ratio and ρ and h represent the mass density and thickness of the plate, respectively.

2.1.4. Functional

Using the Gâteaux differential and Eq. (1), a functional for the free vibration analysis of the Kirchhoff plate–Pasternak foundation system was obtained by Omurtag et al. [5] as

$$\begin{aligned} I=&\iint\left(\frac{\partial K}{\partial x}\frac{\partial w}{\partial x}+\frac{\partial M}{\partial y}\frac{\partial w}{\partial y}+\frac{\partial T}{\partial y}\frac{\partial w}{\partial x}+\frac{\partial T}{\partial x}\frac{\partial w}{\partial y}\right)\mathrm{d}A+\iint\left(-\frac{6}{Gh^3}T^2\right)\mathrm{d}A\\ &+\iint\left(-\frac{6}{Eh^3}(K^2+M^2-2\upsilon KM)\right)\mathrm{d}A-\iint\left(\frac{1}{2}\rho h\omega^2 w^2\right)\mathrm{d}A\\ &+\iint\left[\frac{1}{2}\bar{G}\left(\frac{\partial w}{\partial x}\frac{\partial w}{\partial x}+\frac{\partial w}{\partial y}\frac{\partial w}{\partial y}\right)+\frac{1}{2}kw^2\right]\mathrm{d}A-\left\{\int\bar{G}\left(\frac{\partial w}{\partial x}(w-\hat{w})\mathrm{d}y+\frac{\partial w}{\partial y}(w-\hat{w})\mathrm{d}x\right)\right\}_{\varepsilon_F}\\ &+\left\{\int\bar{G}\left(\frac{\partial \hat{w}}{\partial x}w\,\mathrm{d}y+\frac{\partial \hat{w}}{\partial y}w\,\mathrm{d}x\right)\right\}_{\sigma_F}-\left\{\int\left[\left(\frac{\partial \hat{K}}{\partial x}+\frac{\partial \hat{T}}{\partial y}\right)w\,\mathrm{d}y+\left(\frac{\partial \hat{M}}{\partial y}+\frac{\partial \hat{T}}{\partial x}\right)w\,\mathrm{d}x\right]\right\}_{\sigma_P}\\ &-\left\{\int\left[\left(\frac{\partial K}{\partial x}+\frac{\partial T}{\partial y}\right)(w-\hat{w})\mathrm{d}y+\left(\frac{\partial M}{\partial y}+\frac{\partial T}{\partial x}\right)(w-\hat{w})\mathrm{d}x\right]\right\}_{\varepsilon_P}\\ &-\left\{\int\left[(K-\hat{K})\frac{\partial w}{\partial x}\,\mathrm{d}y+(T-\hat{T})\frac{\partial w}{\partial x}\,\mathrm{d}x+(M-\hat{M})\frac{\partial w}{\partial y}\,\mathrm{d}x+(T-\hat{T})\frac{\partial w}{\partial y}\,\mathrm{d}y\right]\right\}_{\sigma_P}\\ &-\left\{\int\left[K\frac{\partial \hat{w}}{\partial x}\,\mathrm{d}y+T\frac{\partial \hat{w}}{\partial x}\,\mathrm{d}x+M\frac{\partial \hat{w}}{\partial y}\mathrm{d}x+T\frac{\partial \hat{w}}{\partial y}\,\mathrm{d}y\right]\right\}_{\varepsilon_P}, \end{aligned} \tag{5}$$

where the terms $(\ldots)_\sigma$ and $(\ldots)_\varepsilon$ represent the dynamic and the geometric boundary conditions, respectively. The subscripts P and F refer to the plate and the foundation, respectively. The terms defined as $(\cdot\,\hat{\cdot}\,\cdot)$ are valid if and only if the boundary conditions are known; otherwise, they disappear. ω is the natural circular frequency. The functional given in Eq. (5) is suitable for a mixed finite element formulation. Hence

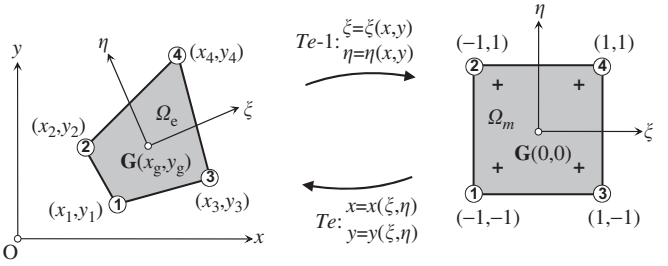

Fig. 4. Quadrilateral isoparametric finite element. *Key:* ○, element nodes; +, Gauss points.

a four-noded isoparametric quadrilateral element with a 2×2 Gauss scheme is used throughout the numerical analysis. As shown in Fig. 4 an arbitrary element Ω_e and master element Ω_m are depicted. An invertible transformation between them exists by means of the maps T_e of Ω_m onto Ω_e by the change of coordinates, and similarly T_e^{-1} is the inverse map from Ω_e to Ω_m. The nodal unknowns are the transverse displacement w, two bending moments K, M and torsional moment T, and their positive directions are shown in Fig. 3. The details of the finite element formulation can be found in Ref. [5].

2.1.5. Calculation of natural frequencies of the plate–foundation system

The natural frequencies of the plate–foundation system are obtained from the solution of a standard eigenvalue problem $[\mathbf{k}]-\omega^2[\mathbf{m}]=0$. By means of the conventional assemblage technique the system matrix $[\mathbf{k}]$ and the mass matrix $[\mathbf{m}]$ for the entire domain are obtained. In the mixed FE analysis, the problem of free vibration yields the following eigenvalue problem:

$$\left(\begin{bmatrix} [\mathbf{k}_{11}] & [\mathbf{k}_{12}] \\ [\mathbf{k}_{12}] & [\mathbf{k}_{22}] \end{bmatrix} - \omega^2 \begin{bmatrix} [\mathbf{0}] & [\mathbf{0}] \\ [\mathbf{0}] & [\mathbf{m}] \end{bmatrix} \right) \begin{Bmatrix} \{\mathbf{f}\} \\ \{\mathbf{w}\} \end{Bmatrix} = \begin{Bmatrix} \{\mathbf{0}\} \\ \{\mathbf{0}\} \end{Bmatrix}, \tag{6}$$

where $\{\mathbf{f}\} = \{\mathbf{K} \quad \mathbf{M} \quad \mathbf{T}\}^{\mathrm{T}}$ and $\{\mathbf{w}\}$ are the stress resultants and the transverse displacement vector, respectively [5]. Elimination of $\{\mathbf{f}\}$ from Eq. (6) yields

$$([\mathbf{k}^*] - \omega^2[\boldsymbol{\mu}])\{\boldsymbol{\omega}\} = \{\mathbf{0}\}, \tag{7}$$

where $[\mathbf{k}^*] = [\mathbf{k}_{22}]-[\mathbf{k}_{12}]^{\mathrm{T}}[\mathbf{k}_{11}]^{-1}[\mathbf{k}_{12}]$ and $[\mathbf{k}^*]$ is the condensed system matrix of the problem and if an interaction problem between the plate and foundation is absent $[\mathbf{k}_{22}] = [\mathbf{0}]$. The element mass matrix is derived using a consistent mass formulation.

2.2. Formulation of fluid–structure interaction problem

2.2.1. Fluid formulation

The fluid is assumed to be ideal, i.e., inviscid and incompressible, and its motion is irrotational and there exists a fluid velocity vector, $\mathbf{v}$, which can be defined as the gradient of the velocity potential function Φ as

$$\mathbf{v}(x, y, z, t) = \nabla\Phi(x, y, z, t), \tag{8}$$

where Φ satisfies Laplace's equation, $\nabla^2\Phi = 0$, throughout the fluid domain.

Before describing the responses of the flexible structure, it is necessary to assign coordinates to the deflections at various degrees of freedom and one particular set of generalized coordinates is the principal coordinate of the *dry* structure (see, for example, Ref. [26]). For a structure vibrating in an ideal fluid, with frequency ω, the principal coordinate, describing the response of the structure in the rth modal vibration, may be expressed by

$$p_r(t) = p_{0r}\, \mathrm{e}^{\mathrm{i}\omega t}. \tag{9}$$

The velocity potential function due to the distortion of the structure in the rth *in vacuo* vibrational mode may be written as follows:

$$\Phi_r(x, y, z, t) = \mathrm{i}\omega\phi_r(x, y, z)p_{0r}\, \mathrm{e}^{\mathrm{i}\omega t}, \quad r = 1, 2, \ldots, N_M, \tag{10}$$

where N_M represents the number of modes of interest and p_{0r} is an unknown amplitude for the rth principal coordinate.

On the wetted surface of the vibrating structure the normal fluid velocity must equal the normal velocity on the structure and this condition for the rth modal vibration of the elastic structure submerged in a quiescent fluid can be expressed as

$$\frac{\partial\phi_r}{\partial n} = \mathbf{u}_r \cdot \mathbf{n}, \tag{11}$$

where $\mathbf{n}$ is the unit normal vector on the wetted surface and points out of the region of interest. The vector $\mathbf{u}_r$ denotes the displacement response of the structure in the rth principal mode and it may be written as

$$\mathbf{u}_r(x, y, z, t) = \mathbf{u}_r(x, y, z)p_{0r}\,\mathrm{e}^{\mathrm{i}\omega t}, \tag{12}$$

where $\mathbf{u}_r$ (x, y, z) is the rth modal displacement vector of the median surface of the plate structure, and it is obtained from the finite element analysis.

It is assumed that the elastic structure vibrates at relatively high frequencies so that the effect of surface waves can be neglected. Therefore, the free surface condition (infinite frequency limit condition) (see, for instance, Ref. [15]) for the perturbation potential can be approximated by

$$\phi_r = 0, \quad \text{on the free surface.} \tag{13}$$

The method of images [23] may be used to satisfy this boundary condition. By adding an imaginary boundary region, the condition given by Eq. (13) at the horizontal surface can be omitted; thus, the problem is reduced to a classical Neumann case.

2.2.2. Numerical evaluation of perturbation potential ϕ

The boundary value problem for the perturbation potential, ϕ, may be expressed in the following form:

$$c(\xi)\phi(\xi) = \iint_{S_W} (\phi^*(s, \xi)q(s) - \phi(s)q^*(s, \xi))\mathrm{d}S, \tag{14}$$

where ξ and s denote, respectively, the evaluation and field points on the wetted surface. S_W denotes the wetted surface of the structure. ϕ^* is the fundamental solution, defined as a solution of the equation $\nabla^2\phi^*(s,\xi) = -\delta(s,\xi)$, where $\delta(s,\xi)$ is the Dirac distribution. It satisfies the Laplace equation everywhere except the evaluation point ξ, and, for a three-dimensional problem, it is expressed as follows:

$$\phi^*(s, \xi) = \frac{1}{4\pi r}. \tag{15}$$

$q = \partial\phi/\partial n$ is the flux and r the distance between the evaluation and field points. The free term $c(\xi)$ is due to the shifting of ξ to the boundary with a limit process and defines the fraction of $\phi(\xi)$ that lies inside the domain of interest. Moreover, $q^*(s,\xi)$ can be written as

$$q^*(s, \xi) = -(\partial r/\partial n)/4\pi r^2. \tag{16}$$

For the solution of Eq. (14) with boundary condition (11), the wetted surface can be idealized by using boundary elements, referred to as hydrodynamic panels, and the distribution of the potential function and its flux over each hydrodynamic panel may be described in terms of the shape functions and nodal values as

$$\phi_e = \sum_{j=1}^{n_e} N_{ej}\phi_{ej}, \quad q_e = \sum_{j=1}^{n_e} N_{ej}q_{ej}. \tag{17}$$

Here, n_e represents the number of nodal points assigned to the eth hydrodynamic panel, and N_{ej} the shape function adopted for the distribution of the potential function. e and j indicate the hydrodynamic panel and nodal point numbers, respectively. For the linear distribution adopted in this study, the shape functions for a quadrilateral panel may be expressed as (see Ref. [27])

$$\begin{aligned} N_{e1} &= ((1-\zeta)(1-\eta))/4, \\ N_{e2} &= ((1+\zeta)(1-\eta))/4, \\ N_{e3} &= ((1+\zeta)(1+\eta))/4, \\ N_{e4} &= ((1-\zeta)(1+\eta))/4 \end{aligned} \tag{18}$$

in the local coordinate system-ζ η shown in Fig. 5. For a quadrilateral panel having 4 nodal points at its corners, n_e takes on the value of 4.

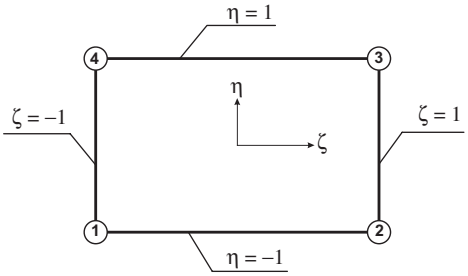

Fig. 5. Quadrilateral boundary element and its local coordinates.

After substituting Eqs. (17) and (18) into Eq. (14) and applying the boundary condition given in Eq. (11), the unknown potential function values can be determined from the following set of algebraic equations:

$$c_k\phi_k + \sum_{i=1}^{N_p}\sum_{j=1}^{n_i}\left(\phi_{i_j}\iint_{\Delta S_i} N_{ij}q^*\,\mathrm{d}S\right) = \sum_{i=1}^{N_p}\sum_{j=1}^{n_i}\left(u_{i_j}n_{i_j}\iint_{\Delta S_i} N_{ij}\phi^*\,\mathrm{d}S\right), \quad k = 1,2,\ldots,m, \tag{19}$$

where m and N_p denote the numbers of nodal points and hydrodynamic panels used in the discretization of the structure. ϕ_{i_j} and $\mathbf{u}_{i_j}$ represent, respectively, the potential value and displacement vector for the jth nodal point of the ith hydrodynamic panel. n_i is the number of nodal points assigned to the ith hydrodynamic panel.

2.2.3. Calculation of generalized fluid–structure interaction forces

Using Bernoulli's equation and neglecting the second-order terms, the dynamic fluid pressure on the elastic structure due to the rth *in-vacuo* modal vibration becomes

$$P_r(x,y,z,t) = -\rho_f\frac{\partial\Phi_r}{\partial t}, \tag{20}$$

where ρ_f is the fluid density. Substituting Eq. (10) into Eq. (20), the following expression for the pressure is obtained:

$$P_r(x,y,z,t) = \rho_f\omega^2\phi_r(x,y,z)p_{0r}\,\mathrm{e}^{\mathrm{i}\omega t}. \tag{21}$$

The kth component of the generalized fluid–structure interaction force due to the rth modal *in-vacuo* vibration of the elastic structure can be expressed in terms of the pressure acting on the wetted surface of the structure as

$$\begin{aligned} Z_{kr} &= \iint_{S_W} P_r(x,y,z,t)\mathbf{u}_k\mathbf{n}\,\mathrm{d}S \\ &= p_{0r}\,\mathrm{e}^{\mathrm{i}\omega t}\iint_{S_W}\rho_f\omega^2\phi_r\mathbf{u}_k\mathbf{n}\,\mathrm{d}S. \end{aligned} \tag{22}$$

The generalized added mass, A_{kr} term, can be defined as

$$A_{kr} = \rho_f\iint_{S_W}\phi_r\mathbf{u}_k\mathbf{n}\,\mathrm{d}S. \tag{23}$$

Therefore, the generalized fluid–structure interaction force component, Z_{kr}, can be written as

$$Z_{kr}(t) = A_{kr}\omega^2 p_{0r}\,\mathrm{e}^{\mathrm{i}\omega t} = -A_{kr}\ddot{p}_r(t). \tag{24}$$

2.2.4. Calculation of wet frequencies and mode shapes

It should be noted that, in the case when a body oscillates in or near a free surface, the hydrodynamic coefficients exhibit frequency dependence in the low-frequency region, but show a tendency towards a constant value in the high-frequency region. In this study, it is assumed that the structure vibrates in the high-frequency region so that the generalized added mass values are constants and evaluated by use of Eq. (23). Hence, the generalized equation of motion for the dynamic fluid–structure interaction system (see, e.g., Ref. [28]), assuming free vibrations with no structural damping, is

$$[-\omega^2(\mathbf{a}+\mathbf{A})+\mathbf{c}]\mathbf{p}=0, \tag{25}$$

where **a** and **c** denote the generalized structural mass and stiffness matrices, respectively. The matrix **A** represents the infinite frequency generalized added mass coefficients.

Solving the eigenvalue problem, expressed by Eq. (25), yields the *wet* frequencies and associated *wet* mode shapes of the structure in contact with fluid. To each *wet* frequency ω_r, there is a corresponding *wet* eigenvector $\mathbf{p}_{0r}=\{p_{r1},p_{r2},\ldots,p_{rm}\}$. The corresponding uncoupled *wet* mode shapes for the structure partially and totally in contact with fluid are obtained as

$$\bar{\mathbf{u}}_r(x,y,z)=\{\bar{u}_r,\bar{v}_r,\bar{w}_r\}=\sum_{j=1}^{N_M}\mathbf{u}_j(x,y,z)\mathbf{p}_{rj}, \tag{26}$$

where $\mathbf{u}_j(x,y,z)=\{u_j,v_j,w_j\}$ denotes the *in vacuo* mode shapes of the *dry* plate structure resting on an elastic foundation and N_M the number of modes included in the analysis. It should be noted that the fluid–structure interaction forces associated with the inertial effect of the fluid do not have the same spatial distribution as those of the *in vacuo* modal forms. Consequently, this produces a hydrodynamic coupling between the *in vacuo* modes of the plate structure with the elastic foundation. This coupling effect is introduced into Eq. (25) through the generalized added mass matrix **A**.

3. Numerical results

A series of calculations have been performed in order to demonstrate the applicability of the method of analysis to vibrating plate structures resting on an elastic foundation and partially in contact with a quiescent fluid. A schematic view of the foundation–structure–fluid interaction system is shown in Fig. 1. The plate chosen is $L=10\,\text{m}$ long, $a=10\,\text{m}$ wide and $h=0.15\,\text{m}$ thick. The plate structure under investigation is made of concrete and has the following material characteristics: Young's modulus $E_s=25\,\text{GPa}$, Poisson's ratio $\upsilon_s=0.15$ and mass density $\rho_s=2400\,\text{kg/m}^3$. For the numerical study, the plate was assumed to be either simply supported or clamped along its four edges.

In this study, the calculations were performed separately for three different soil types: clay with Young's modulus $E_f=50\,\text{MPa}$, Poisson's ratio $\upsilon_f=0.45$ and soil stiffness $k_f=15\,\text{MN/m}^3$ (weak foundation); sand and gravel with $E_f=200\,\text{MPa}$, $\upsilon_f=0.25$ and $k_f=150\,\text{MN/m}^3$ (medium hard foundation); and shale with $E_f=2500\,\text{MPa}$, $\upsilon_f=0.2$ and $k_f=2000\,\text{MN/m}^3$ (hard foundation). Furthermore, it was assumed that the structure was resting on a Pasternak-type foundation and partially in contact with fresh water with a density of $1000\,\text{kg/m}^3$ (see Fig. 1).

The mode shapes of rectangular plate structures may be identified with two integers, such as i and j. These integers, i and j, are considered as the number of half-waves along the length and width of the plate structure, respectively, and a combination of i and j forms a particular mode shape.

3.1. Idealization and convergence

The *in vacuo* dynamic characteristics (natural frequencies and associated mode shapes) of the plate structure resting on a Pasternak foundation were obtained by using the aforementioned mixed finite element analysis. The plate finite element PLTVE4 [5] was adopted in this study, and it is an isoparametric conforming C^0 class element having four corner nodes and at each node four degrees of freedom are present (one transverse

Table 1
Convergence of *dry* natural frequencies (Hz) for a plate structure resting on a hard foundation (shale) and clamped along its edges

Mode (*i*,*j*)	64 elements	144 elements	256 elements	400 elements
1,1	394.3	394.3	394.3	394.3
1,2	423.0	422.1	421.8	421.8
2,1	423.0	422.1	421.8	421.8
2,2	449.9	448.2	447.8	447.6
3,1	471.4	466.8	465.4	464.8
1,3	471.4	466.8	465.4	464.8
2,3	495.8	490.8	489.2	488.6
3,2	495.8	490.8	489.2	488.6
4,1	540.4	527.2	522.8	520.9
1,4	540.4	527.2	522.8	520.9

Table 2
Convergence of *dry* natural frequencies (Hz) for a plate structure resting on a weak foundation (clay) and simply supported along its edges

Mode (*i*,*j*)	64 elements	144 elements	256 elements	400 elements
1,1	36.34	36.29	36.29	36.29
1,2	42.63	42.38	42.28	42.23
2,1	42.63	42.38	42.28	42.23
2,2	49.07	48.62	48.47	48.37
3,1	54.56	53.35	52.95	52.75
1,3	54.71	53.40	52.95	52.75
2,3	61.15	59.79	59.29	59.09
3,2	61.15	59.79	59.29	59.09
4,1	74.44	70.36	68.95	68.30
1,4	74.44	70.36	68.95	68.30

displacement, two bending moments and one torsional moment). Therefore, a total number of 16 degrees of freedom are assigned to each element.

A series of calculations were performed in order to test the convergence of the finite element calculations (natural frequencies and associated mode shapes). The results of the finite element convergence test studies are presented in Tables 1 and 2 for two different edge conditions and foundation types. Table 1 presents the natural frequencies of the plate structure resting on a hard foundation (shale) and clamped along its edges, and Table 2 those of the plate structure resting on a weak foundation (clay) and simply supported along its edges. In the tables, the results are presented for four different finite element idealizations. In the first group of idealizations, the distributions over the plates consist of eight equally spaced elements along the length and width of the plate structure. Therefore, a total number of 64 elements were distributed over the plate. To test the convergence of the calculated dynamic properties, the number of elements over the plate was increased first to 144 (12 elements along the length and width) and then to 256 (16 elements along the length and width). In the final test of idealizations, the number of elements was increased to 20 along the length and width of the plate, and therefore a total number of 400 elements were distributed over the structure in this final idealization. The differences in the results presented in Tables 1 and 2 indicate that the calculated natural frequency values are converging with increasing number of elements. It can be observed from Table 2 that, for the plate structure resting on a weak foundation (clay) with simply supported edges, all the natural frequency values are converged satisfactorily for the last two idealizations. On the other hand, for the plate on a hard foundation (shale) with clamped edges, the differences between the last two idealizations are considerable small for the mode shapes presented, as seen from Table 1. The results of the final idealizations (400 elements) were adopted for the *in vacuo* dynamic properties of the plate–foundation system. It should also be noted that the *in vacuo* dynamic characteristics (mode shapes, etc.) are scaled to a generalized mass of 1 kgm^2.

Table 3
Convergence of *wet* natural frequencies (Hz) for a plate structure resting on a hard foundation (shale) and clamped along its edges (submerging depth ratio, $H/L = 1.0$)

Mode (*i,j*)	64 panels	144 panels	256 panels	400 panels
1,1	126.1	126.5	126.7	126.9
1,2	170.4	172.1	172.7	173.1
2,1	175.2	177.1	177.8	178.2
2,2	203.6	207.4	208.8	209.5
1,3	217.1	220.7	222.0	222.7
3,1	222.4	226.7	228.2	228.9
2,3	241.1	247.7	250.0	251.1
3,1	242.9	249.9	252.3	253.4
1,4	268.5	274.8	276.7	277.7
4,1	272.1	279.8	282.0	283.1

Table 4
Convergence of *wet* natural frequencies (Hz) for a plate structure resting on a weak foundation (clay) and simply supported along its edges (submerging depth ratio, $H/L = 0.5$)

Mode (*i,j*)	32 panels	72 panels	128 panels	200 panels
1,1	16.47	16.47	16.46	16.46
1,2	21.34	21.45	21.48	21.48
2,1	29.02	29.19	29.19	29.19
2,2	31.96	31.20	30.90	30.75
1,3	36.62	36.15	35.90	35.77
3,1	40.53	40.58	40.44	40.36
2,3	41.35	41.16	41.05	40.99
3,1	44.22	44.34	44.18	44.07
1,4	47.41	47.16	47.02	46.93
4,1	58.50	55.63	54.45	53.88

To test the convergence of the boundary element calculations (hydrodynamic predictions), various numbers of hydrodynamic panels (boundary elements) were distributed over the wetted surface of the plate. The main aim of this exercise was to represent accurately the distortional mode shapes of the wetted surface area of the plate. The results of the *wet* convergence studies are given in Tables 3 and 4, respectively, for the plate resting on the hard (shale) and weak (clay) foundations. The results in Tables 3 and 4 are calculated, respectively, for the submerging depth ratios $H/L = 1$ and 0.5. Furthermore, for the results presented in Tables 3 and 4, the plate structure is, respectively, clamped and simply supported along all its edges. Four different idealizations were considered over the wetted surface of the plate structure. The hydrodynamic panels were distributed over the wetted surface as follows: one structural element (finite element) corresponding to one hydrodynamic panel. Therefore, the same number of hydrodynamic panels and structural elements were adopted for the *wet* results presented for the submerging depth ratio $H/L = 1$ in Table 3. Therefore, 64, 144, 256 and 400 hydrodynamic panels were distributed over the wetted surface, respectively, for four idealizations considered in Table 3. It can be observed from the table that the *wet* frequency values converge with increasing number of hydrodynamic panels. The frequency values of the final idealization (400 panels) may be assumed as reasonably converged. For the plate simply supported along its edges with the submerging depth ratio $H/L = 0.5$ and resting on a weak foundation (clay), 32, 72, 128 and 200 hydrodynamic panels were distributed over the wetted surface separately for four different idealization. For these idealizations the hydrodynamic panels are distributed along the length and width, respectively, as follows: 4 and 8 (32 panels); 6 and 12 (72 panels); 8 and 16 (128 panels); and 10 and 20 (200 panels). It can be observed from Table 4 that the *wet* frequencies are converging fast with increasing number of hydrodynamic panels. The differences between the last two idealizations (128 and 200 hydrodynamic panel idealizations) are reasonably small for all the modes given in Table 4. For all the results presented in this study, 80, 160, 240, 320 and 400 hydrodynamic panels

were adopted for the plate with the submerging depth ratios, $H/L = 0.2$, 0.4, 0.6, 0.8 and 1, respectively. On the other hand, an additional convergence study was also carried out to establish the number of distortional modes needed for the predictions. As a result of this analysis, 40 *in vacuo* modes were included in the calculations presented in this study.

3.2. Numerical calculations

By solving the eigenvalue problem, Eq. (25), the uncoupled modes and associated frequencies of the plate resting on a foundation and partially submerged in a quiescent fluid were obtained for two different edge support conditions, i.e., simply supported and clamped edge conditions. It should be mentioned that the finite element method adopted in this study was successfully employed before and verified with the analytical results found in the literature (see Ref. [5]). On the other hand, the fluid–structure interaction approach used was also successfully employed for the problems of fluid-containing shell structures and also for cantilever plates partially submerged in fluid (see, for example, Ref. [15,23]). Unfortunately, for this study, there is no result available for comparison purposes. It is expected that the results presented here may serve as a benchmark for future studies on the subject. Furthermore, the non-dimensional frequency values presented in Tables 5 and 6 are calculated according to the following expression: $\Omega = \omega a^2(\rho_s h/D)^{1/2}$, where ω is the circular frequency in Hz and D the flexural rigidity and defined as $D = Eh^3/12(1-\upsilon^2)$. a, h and ρ_s are, respectively, the width, thickness and density of the plate considered.

The calculated non-dimensional *dry* and *wet* natural frequencies are presented in Table 5 for the plate structure with or without a foundation and partially in contact with fresh water. The effects of various foundation types were considered, and the results are presented for weak (clay), medium hard (sand and gravel) and hard (shale) foundations, and for simply supported edge conditions. As can be observed from Table 5, the non-dimensional natural frequency values are given for the submerging depth ratios, $H/L = 0$,

Table 5
Non-dimensional frequency values for a plate structure simply supported along its edges

Mode (*i*,*j*)	*H*/*L*						Mode (*i*,*j*)	*H*/*L*					
	0.0	0.2	0.4	0.6	0.8	1.0		0.0	0.2	0.4	0.6	0.8	1.0
	No foundation							Weak foundation					
1,1	3.169	3.064	2.196	1.496	1.173	1.036	1,1	25.67	22.63	13.46	10.49	9.098	8.315
2,1	7.902	7.092	5.708	5.174	3.926	3.337	2,1	29.88	26.86	25.62	18.38	14.49	12.63
1,2	7.902	7.622	5.382	4.058	3.484	3.261	1,2	29.88	26.38	16.96	14.12	12.90	12.29
2,2	12.68	11.40	9.974	8.746	6.777	5.942	2,2	34.22	31.05	29.59	21.83	17.83	16.03
3,1	15.95	13.80	12.57	10.57	9.410	7.848	3,1	37.32	33.34	29.82	28.16	21.82	18.36
1,3	15.99	15.25	10.65	8.750	7.951	7.623	1,3	37.32	32.68	22.47	19.63	18.42	17.84
3,1	20.69	18.10	16.68	14.47	12.66	10.72	3,2	41.80	37.70	33.91	32.07	25.23	21.67
2,3	20.69	18.64	17.52	14.57	11.74	10.63	2,3	41.80	38.41	36.33	27.42	23.29	21.47
4,1	27.52	24.21	21.36	19.32	17.66	14.91	4,1	48.32	43.74	39.32	34.62	31.62	26.22
1,4	27.52	25.66	18.31	15.96	15.00	14.62	1,4	48.32	41.80	30.45	27.43	26.23	25.70
	Medium hard foundation							Hard foundation					
1,1	76.48	57.46	36.68	30.01	26.65	24.59	1,1	278.8	203.2	132.5	109.0	96.93	89.51
2,1	82.14	77.33	62.77	46.26	38.85	34.68	2,1	297.9	281.3	219.5	165.5	140.3	125.7
1,2	82.14	62.76	43.22	37.59	35.05	33.68	1,2	297.9	220.2	155.2	135.8	126.9	122.0
2,2	87.66	82.98	67.81	51.71	44.64	40.99	2,2	315.9	300.3	219.5	183.7	160.2	147.6
3,1	91.47	85.20	79.06	65.48	51.82	45.02	3,1	327.9	306.8	286.2	227.7	184.0	161.3
1,3	91.47	70.71	51.92	47.11	44.86	43.77	1,3	327.9	244.5	184.0	168.3	160.5	156.8
3,2	96.85	90.69	84.61	69.89	56.79	50.19	3,1	344.4	324.4	304.6	242.2	200.0	178.4
2,3	96.85	92.27	75.29	59.59	52.99	49.72	2,3	344.4	330.1	256.1	208.6	187.6	176.8
4,1	104.5	97.58	90.26	82.24	67.11	56.74	4,1	367.0	344.6	317.9	288.8	232.4	199.3
1,4	104.5	81.96	62.89	58.35	56.45	55.62	1,4	367.0	278.0	218.3	204.1	198.1	195.4

Table 6
Non-dimensional frequency values for a plate structure clamped along its edges

Mode (i,j)	H/L						Mode (i,j)	H/L					
	0.0	0.2	0.4	0.6	0.8	1.0		0.0	0.2	0.4	0.6	0.8	1.0
	No foundation							Weak foundation					
1,1	5.730	5.674	4.202	2.747	2.157	1.948	1,1	26.42	25.43	14.84	11.18	9.57	8.75
2,1	11.75	11.18	8.590	7.606	5.754	5.101	2,1	31.65	28.94	27.13	19.77	15.39	13.61
1,2	11.75	11.60	8.254	6.109	5.282	5.023	1,2	31.65	30.26	18.88	15.37	13.95	13.34
2,2	17.27	16.34	13.84	11.84	9.164	8.300	2,2	36.85	33.82	32.04	23.82	19.30	17.57
3,1	21.26	19.10	16.78	14.47	12.31	10.64	3,1	40.55	36.23	32.50	29.97	23.43	20.21
1,3	21.36	20.89	14.42	11.76	10.71	10.27	1,3	40.59	38.10	25.16	21.71	20.30	19.67
3,2	26.49	23.85	21.43	18.94	15.96	13.94	3,2	45.64	41.18	37.23	34.80	27.33	23.95
2,3	26.49	24.81	22.78	18.51	14.97	13.85	2,3	45.64	42.17	40.17	30.47	25.55	23.79
4,1	34.54	30.29	26.84	24.21	21.89	18.80	4,1	53.33	47.79	34.20	38.03	34.38	29.11
1,4	34.54	33.28	23.21	20.08	18.90	18.49	1,4	53.33	48.85	42.98	30.57	29.19	28.65
	Medium hard foundation							Hard foundation					
1,1	76.91	62.23	37.95	30.67	27.12	25.01	1,1	279.0	205.8	133.2	109.3	97.20	89.75
2,1	83.17	77.88	65.39	47.51	39.59	35.42	2,1	298.4	281.6	220.9	166.2	140.7	126.1
1,2	83.17	67.84	44.82	38.63	35.93	34.53	1,2	298.4	222.9	156.0	136.3	127.4	122.5
2,2	89.27	84.11	70.87	53.32	45.78	42.14	2,2	316.7	300.8	236.6	184.5	160.8	148.2
3,1	93.43	86.52	79.90	67.47	52.97	46.29	3,1	328.8	307.5	286.6	228.8	184.7	162.0
1,3	93.43	76.28	54.01	48.66	46.27	45.14	1,3	328.8	247.4	185.1	169.1	161.3	157.5
3,2	99.30	92.57	86.00	72.34	58.21	51.83	3,2	345.7	325.3	305.3	243.5	200.8	179.3
2,3	99.30	94.30	78.74	61.71	54.68	51.44	2,3	345.7	331.1	257.9	209.8	188.5	177.7
4,1	107.7	99.98	92.51	83.90	68.82	58.75	4,1	368.5	345.8	319.3	289.8	233.2	200.3
1,4	107.7	88.44	65.65	60.65	58.72	57.78	1,4	368.5	281.5	219.7	205.3	199.2	196.5

0.2, 0.4, 0.6, 0.8 and 1, and the lowest non-dimensional frequency values are obtained for the plate with no foundation. It can also be realized that the *wet* frequencies increase with increasing hardness of foundation for a specific mode shape and submerging depth ratio. For instance, for the first mode shape ($i = 1$, $j = 1$) and submerging depth ratio $H/L = 0.4$, the non-dimensional *wet* frequency of the plate structure takes on the values of 13.46, 36.68 and 132.5, respectively, for the weak, medium hard and hard foundation types. On the other hand, it can be seen that the frequencies decrease with increasing submerging depth, and therefore the lowest frequency values were obtained for the submerging depth ratio $H/L = 1$.

The calculations were repeated for clamped edge conditions, and these results are presented in Table 6. By comparing the non-dimensional frequency values in Tables 5 and 6, it can be observed that all the frequencies of the plate structure with clamped edges are higher in comparison with the corresponding ones of the plate with simply supported edges. Meanwhile, the observations made previously for the plate with simply supported edges can also be repeated here for the plate with clamped edges. That is to say, the frequency values increase with increasing hardness of the foundation, and that they decrease with increasing submerging depth ratio.

Tables 7 and 8 show the calculated generalized added masses for the plate structure, respectively, with simply supported and clamped edges. Those results presented in Tables 7 and 8 are the generalized added mass parameters, $\bar{A}_{kr}$, and they are defined as $\bar{A}_{kr} = A_{kr}(\rho_f a/\rho_s h) \times 100$, where A_{kr} is the kth generalized added mass term due to the vibration in the rth *in vacuo* mode. The added mass parameters for the first eight distortional *in vacuo* modes are presented for the submerging depth ratios $H/L = 0.2$, 0.6 and 1.0, and for weak, medium hard and hard foundation types. The added mass values correspond to a generalized structural mass of 1 kg m^2. Here, it is assumed that the structure preserves its *in vacuo* principal mode shapes in the fluid and that each mode gives rise to the surface pressure distribution of the flexible structure. However, the hydrodynamic forces associated with the inertial effect of the surrounding fluid medium do not necessarily have the same spatial distribution as those of the *in vacuo* principal modes. Consequently, this produces

Table 7
Generalized added mass parameters of a plate structure simply supported along its edges

Mode (i,j)	Weak foundation								Medium hard foundation								Hard foundation							
	1,1	2,1	1,2	2,2	3,1	1,3	3,2	2,3	1,1	2,1	1,2	2,2	3,1	1,3	3,2	2,3	1,1	2,1	1,2	2,2	3,1	1,3	3,2	2,3
	$H/L = 0.2$								$H/L = 0.2$								$H/L = 0.2$							
1,1	0.236	0.438	−0.005	0.000	0.405	0.410	0.000	−0.005	0.236	0.436	0.042	0.000	−0.405	−0.410	0.000	0.006	0.236	−0.433	0.067	0.000	0.406	−0.411	−0.001	0.007
2,1	0.438	0.812	−0.006	0.004	0.753	0.762	−0.005	−0.010	0.436	0.807	0.057	−0.038	−0.750	−0.759	−0.050	0.011	−0.433	0.799	−0.091	−0.061	−0.744	0.754	0.081	0.002
1,2	−0.005	−0.006	0.214	0.397	−0.008	−0.008	−0.521	−0.028	0.042	0.057	0.220	0.396	−0.072	−0.073	0.521	0.004	0.067	−0.091	0.229	−0.394	0.116	−0.117	0.509	0.097
2,2	0.000	0.004	0.397	0.735	0.000	0.000	−0.967	−0.051	0.000	−0.038	0.396	0.737	0.000	0.000	0.971	0.005	0.000	−0.061	−0.394	0.739	0.000	0.000	−0.956	−0.178
3,1	0.405	0.753	−0.008	0.000	0.797	0.612	−0.013	0.244	−0.405	−0.750	−0.072	0.000	0.797	0.612	−0.001	0.243	0.406	−0.744	0.116	0.000	0.797	−0.612	0.044	−0.238
1,3	0.410	0.762	−0.008	0.000	0.612	0.813	0.014	−0.261	−0.410	−0.759	−0.073	0.000	0.612	0.815	0.001	−0.265	−0.411	0.754	−0.117	0.000	−0.612	0.816	0.049	−0.263
3,2	0.000	−0.005	−0.521	−0.967	−0.013	0.014	1.278	0.033	0.000	−0.050	0.521	0.971	−0.001	0.001	1.281	0.003	−0.001	0.081	0.509	−0.956	0.044	0.049	1.262	0.111
2,3	−0.005	−0.010	−0.028	−0.051	0.244	−0.261	0.033	0.664	0.006	0.011	0.004	0.005	0.243	−0.265	0.003	0.665	0.007	0.002	0.097	−0.178	−0.238	−0.263	0.111	0.688
	$H/L = 0.6$								$H/L = 0.6$								$H/L = 0.6$							
1,1	11.52	9.405	−0.100	0.000	0.138	1.187	0.040	−0.752	11.52	9.364	0.900	0.000	−0.138	−1.187	−0.004	0.749	11.52	−9.297	1.444	0.000	0.138	−1.188	−0.137	0.735
2,1	9.405	10.38	−0.021	0.067	2.956	4.009	0.044	−0.795	9.364	10.37	0.191	−0.608	−2.942	−3.992	0.009	0.793	−9.297	10.34	−0.304	−0.975	−2.920	3.965	0.123	−0.779
1,2	−0.100	−0.021	8.378	6.347	−0.031	−0.043	0.143	0.016	0.900	0.191	8.397	6.321	−0.283	−0.384	−0.142	0.075	1.444	−0.304	8.426	−6.276	0.453	−0.616	−0.160	0.095
2,2	0.000	0.067	6.347	7.136	0.000	0.000	−3.386	−0.180	0.000	−0.608	6.321	7.138	0.000	0.000	3.392	0.018	0.000	−0.975	−6.276	7.139	0.000	0.000	−3.336	−0.620
3,1	0.138	2.956	−0.031	0.000	6.544	0.356	−0.161	3.038	−0.138	−2.942	−0.283	0.000	6.544	0.356	−0.016	3.039	0.138	−2.920	0.453	0.000	6.544	−0.357	0.555	−2.986
1,3	1.187	4.009	−0.043	0.000	0.356	7.148	0.189	−3.569	−1.187	−3.992	−0.384	0.000	0.356	7.149	0.019	−3.579	−1.188	3.965	−0.616	0.000	−0.357	7.150	0.655	−3.523
3,2	0.040	0.044	0.143	−3.386	−0.161	0.189	5.933	0.029	−0.004	0.009	−0.142	3.392	−0.016	0.019	5.936	0.003	−0.137	0.123	−0.160	−3.336	0.555	0.655	5.920	0.097
2,3	−0.752	−0.795	0.016	−0.180	3.038	−3.569	0.029	5.394	0.749	0.793	0.075	0.018	3.039	−3.579	0.003	5.394	0.735	−0.779	0.095	−0.620	−2.986	−3.523	0.097	5.413
	$H/L = 1.0$								$H/L = 1.0$								$H/L = 1.0$							
1,1	29.99	2.942	−0.031	0.000	−0.822	3.857	0.036	−0.684	30.00	2.931	0.282	0.000	0.822	−3.856	−0.004	0.688	30.00	−2.910	0.452	0.000	−0.822	−3.856	−0.126	0.678
2,1	2.942	16.83	0.007	0.007	0.619	1.593	0.042	−0.910	2.931	16.84	−0.064	−0.063	−0.616	−1.587	−0.057	0.906	−2.910	16.85	0.102	−0.101	−0.612	1.577	0.247	−0.870
1,2	−0.031	0.007	17.50	0.656	−0.007	−0.017	−0.547	−0.019	0.282	−0.064	17.50	0.655	−0.059	−0.153	0.545	0.090	0.452	0.102	17.49	−0.651	0.095	−0.245	0.508	0.237
2,2	0.000	0.007	0.656	12.80	0.000	0.000	−0.568	−0.030	0.000	−0.063	0.655	12.80	0.000	0.000	0.570	0.003	0.000	−0.101	−0.651	12.80	0.000	0.000	−0.562	−0.104
3,1	−0.822	0.619	−0.007	0.000	11.55	−0.443	−0.002	0.046	0.822	−0.616	−0.059	0.000	11.55	−0.443	0.000	0.046	−0.822	−0.612	0.095	0.000	11.55	0.443	0.008	−0.045
1,3	3.857	1.593	−0.017	0.000	−0.443	12.50	0.023	−0.437	−3.856	−1.587	−0.153	0.000	−0.443	12.50	0.002	−0.440	−3.856	1.577	−0.245	0.000	0.443	12.50	0.081	−0.434
3,2	0.036	0.042	−0.547	−0.568	−0.002	0.023	9.823	−0.015	−0.004	−0.057	0.545	0.570	0.000	0.002	9.824	−0.001	−0.126	0.247	0.508	−0.562	0.008	0.081	9.836	−0.049
2,3	−0.684	−0.910	−0.019	−0.030	0.046	−0.437	−0.015	10.10	0.688	0.906	0.090	0.003	0.046	−0.440	−0.001	10.10	0.678	−0.870	0.237	−0.104	−0.045	−0.434	−0.049	10.09

Table 8
Generalized added mass parameters of a plate structure clamped along its edges

Mode (i,j)	Weak foundation								Medium hard foundation								Hard foundation							
	1,1	1,2	2,1	2,2	3,1	1,3	2,3	3,2	1,1	1,2	2,1	2,2	3,1	1,3	2,3	3,2	1,1	1,2	2,1	2,2	3,1	1,3	2,3	3,2
	$H/L = 0.2$								$H/L = 0.2$								$H/L = 0.2$							
1,1	0.113	−0.013	0.222	0.000	0.223	0.226	−0.002	0.000	0.163	−0.019	0.308	0.000	0.296	0.300	−0.005	0.000	0.223	−0.013	0.415	0.000	0.386	0.391	−0.006	−0.002
1,2	−0.013	0.111	−0.019	−0.214	−0.026	−0.026	−0.004	−0.302	−0.019	0.153	−0.026	−0.285	−0.034	−0.035	0.027	−0.386	−0.013	0.204	−0.018	0.378	−0.023	−0.023	0.179	−0.466
2,1	0.222	−0.019	0.437	−0.013	0.439	0.447	−0.006	−0.018	0.308	−0.026	0.583	−0.017	0.559	0.567	−0.008	−0.024	0.415	−0.018	0.771	0.012	0.718	0.728	−0.006	−0.019
2,2	0.000	−0.214	−0.013	0.418	0.000	0.000	0.009	0.592	0.000	−0.285	−0.017	0.539	0.000	0.000	−0.051	0.731	0.000	0.378	0.012	0.702	0.000	0.000	0.332	−0.867
3,1	0.223	−0.026	0.439	0.000	0.494	0.397	0.137	−0.002	0.296	−0.034	0.559	0.000	0.607	0.475	0.175	0.012	0.386	−0.023	0.718	0.000	0.763	0.587	0.215	0.082
1,3	0.226	−0.026	0.447	0.000	0.397	0.516	−0.158	0.002	0.300	−0.035	0.567	0.000	0.475	0.624	−0.197	−0.014	0.391	−0.023	0.728	0.000	0.587	0.781	−0.238	−0.091
2,3	−0.002	−0.004	−0.006	0.009	0.137	−0.158	0.403	0.007	−0.005	0.027	−0.008	−0.051	0.175	−0.197	0.500	−0.035	−0.006	0.179	−0.006	0.332	0.215	−0.238	0.712	−0.199
3,2	0.000	−0.302	−0.018	0.592	−0.002	0.002	0.007	0.842	0.000	−0.386	−0.024	0.731	0.012	−0.014	−0.035	0.996	−0.002	−0.466	−0.019	−0.867	0.082	−0.091	−0.199	1.154
	$H/L = 0.6$								$H/L = 0.6$								$H/L = 0.6$							
1,1	11.02	−0.515	8.742	0.000	−0.024	1.221	−0.809	0.012	11.25	−0.554	9.049	0.000	0.046	1.162	−0.774	−0.054	11.48	−0.293	9.347	0.000	0.123	1.180	−0.702	−0.269
1,2	−0.515	8.052	−0.099	−5.907	−0.162	−0.237	0.056	0.207	−0.554	8.195	−0.112	−6.099	−0.174	−0.242	0.037	0.196	−0.293	8.349	−0.062	6.308	−0.092	−0.125	−0.031	0.150
2,1	8.742	−0.099	9.734	−0.348	2.754	4.028	−0.892	0.026	9.049	−0.112	10.01	−0.374	2.834	3.952	−0.828	−0.046	9.347	−0.062	10.32	0.197	2.934	3.997	−0.749	−0.282
2,2	0.000	−5.907	−0.348	6.722	0.000	0.000	0.050	3.294	0.000	−6.099	−0.374	6.894	0.000	0.000	−0.229	3.305	0.000	6.308	0.197	7.097	0.000	0.000	1.210	−3.154
3,1	−0.024	−0.162	2.754	0.000	6.319	0.329	2.814	−0.043	0.046	−0.174	2.834	0.000	6.404	0.340	2.907	0.202	0.123	−0.092	2.934	0.000	6.519	0.354	2.816	1.080
1,3	1.221	−0.237	4.028	0.000	0.329	7.004	−3.474	0.053	1.162	−0.242	3.952	0.000	0.340	7.029	−3.485	−0.242	1.180	−0.125	3.997	0.000	0.354	7.127	−3.329	−1.277
2,3	−0.809	0.056	−0.892	0.050	2.814	−3.474	5.176	0.008	−0.774	0.037	−0.828	−0.229	2.907	−3.485	5.249	−0.039	−0.702	−0.031	−0.749	1.210	2.816	−3.329	5.438	−0.183
3,2	0.012	0.207	0.026	3.294	−0.043	0.053	0.008	5.737	−0.054	0.196	−0.046	3.305	0.202	−0.242	−0.039	5.811	−0.269	0.150	−0.282	−3.154	1.080	−1.277	−0.183	5.846
	$H/L = 1.0$								$H/L = 1.0$								$H/L = 1.0$							
1,1	28.48	−0.135	2.287	0.000	−0.613	4.810	−0.641	0.010	29.23	−0.157	2.565	0.000	−0.694	4.247	−0.652	−0.045	29.87	−0.090	2.878	0.000	−0.798	3.913	−0.638	−0.245
1,2	−0.135	16.49	0.029	−0.446	−0.026	−0.080	0.050	−0.852	−0.157	16.94	0.035	−0.527	−0.031	−0.087	0.108	−0.695	−0.090	17.41	0.020	0.634	−0.019	−0.049	0.233	−0.526
2,1	2.287	0.029	15.99	−0.026	0.435	1.360	−1.062	−0.034	2.565	0.035	16.38	−0.032	0.503	1.427	−0.962	−0.110	2.878	0.020	16.76	0.020	0.597	1.562	−0.852	−0.346
2,2	0.000	−0.446	−0.026	12.18	0.000	0.000	0.006	0.393	0.000	−0.527	−0.032	12.45	0.000	0.000	−0.031	0.452	0.000	0.634	0.020	12.74	0.000	0.000	0.196	−0.512
3,1	−0.613	−0.026	0.435	0.000	11.01	−0.367	0.001	0.000	−0.694	−0.031	0.503	0.000	11.23	−0.387	0.017	0.001	−0.798	−0.019	0.597	0.000	11.50	−0.432	0.038	0.014
1,3	4.810	−0.080	1.360	0.000	−0.367	12.45	−0.418	0.006	4.247	−0.087	1.427	0.000	−0.387	12.36	−0.409	−0.028	3.913	−0.049	1.562	0.000	−0.432	12.47	−0.406	−0.156
2,3	−0.641	0.050	−1.062	0.006	0.001	−0.418	9.705	−0.003	−0.652	0.108	−0.962	−0.031	0.017	−0.409	9.847	0.016	−0.638	0.233	−0.852	0.196	0.038	−0.406	10.02	0.089
3,2	0.010	−0.852	−0.034	0.393	0.000	0.006	−0.003	9.498	−0.045	−0.695	−0.110	0.452	0.001	−0.028	0.016	9.622	−0.245	−0.526	−0.346	−0.512	0.014	−0.156	0.089	9.826

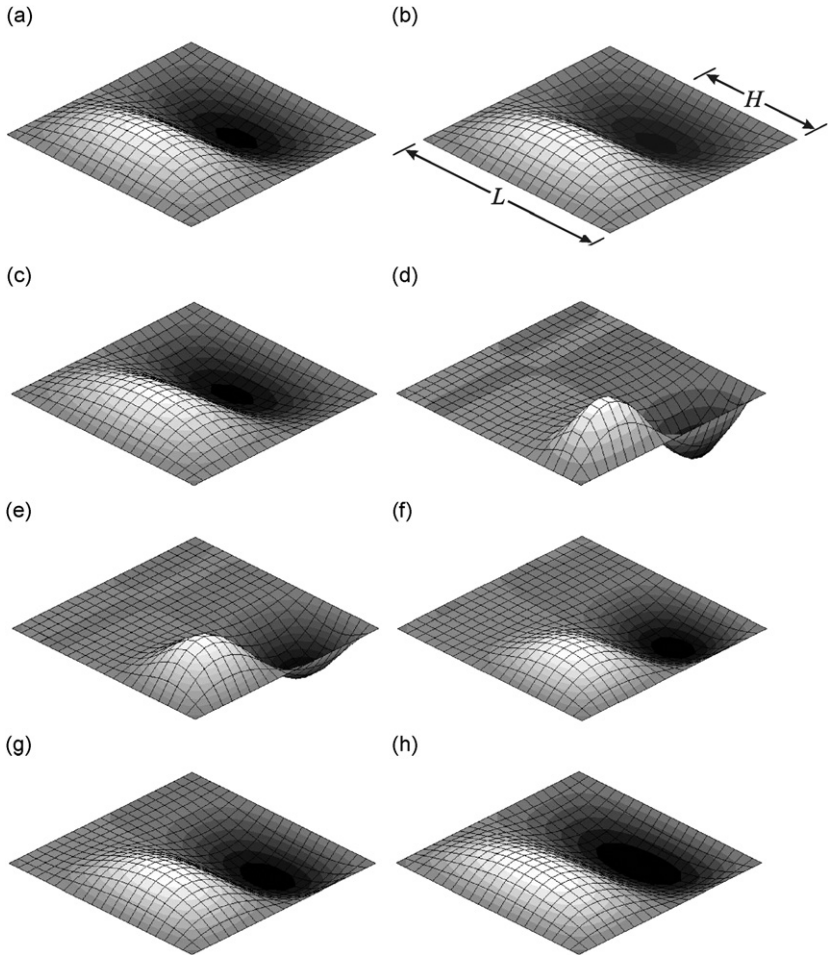

Fig. 6. Mode shape ($i = 1$, $j = 2$) for a plate simply supported along its edges. No foundation: (a) $H/L = 0.0$; (b) $H/L = 0.6$. Medium hard foundation (sand and gravel): (c) $H/L = 0.0$; (d) $H/L = 0.2$; (e) $H/L = 0.4$; (f) $H/L = 0.6$; (g) $H/L = 0.8$; (h) $H/L = 1.0$.

hydrodynamic coupling between the *in vacuo* modes. As can be seen from Tables 7 and 8, there is strong hydrodynamic coupling between some of the *in vacuo* modes. It can also be observed from Tables 7 and 8 that the generalized added mass matrices are symmetric and the cross-coupling terms are generally small in comparison with the diagonal ones. On the other hand, it can be realized that the coupling effects generally become stronger for small submerging depths. For instance, the ratios of the cross-coupling terms to corresponding diagonal terms are mainly larger for the submerging depth ratio $H/L = 0.2$ when compared with the fully submerged plate (depth ratio $H/L = 1.0$).

Fig. 6 shows the mode shape (1, 2) for various submerging depths and simply supported edge conditions. The calculations were performed for the plate structure with no foundation and medium hard foundation (sand and gravel). For the case of no foundation, the mode shape (2, 1) is presented for the submerging depth ratios $H/L = 0.0$ and 0.6 (see Figs. 6 (a) and (b)). Moreover, for those in Figs. 6 (c)–(h), the plate structure was resting on the medium hard foundation with the submerging depth ratios, H/L, 0.0, 0.2, 0.4, 0.6, 0.8 and 1, respectively. As can be seen from Fig. 6 (b), the *in vacuo* mode shape is more or less preserved when the plate is submerged with the depth ratio, $H/L = 0.6$. Furthermore, for the plate with a medium hard foundation and lower depth ratios such as $H/L = 0.2$ and 0.4, the *wet* part of the plate structure shows high levels of vibration. The larger area of the plate indulges into vibration as the depth ratio, H/L, increases. For the fully submerged case, $H/L = 1.0$, the modal vibration form resembles like the corresponding *in vacuo* modal form.

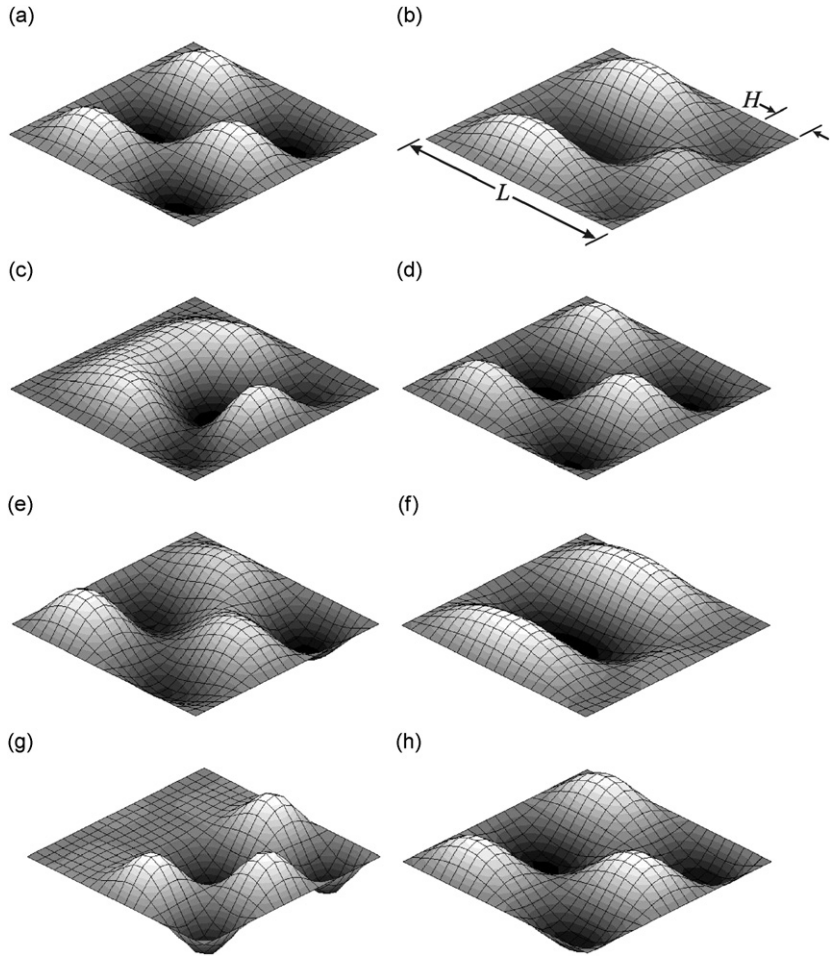

Fig. 7. Mode shape ($i = 2$, $j = 3$) for a plate clamped along its edges. Weak foundation (clay): (a) $H/L = 0.0$; (b) $H/L = 0.2$; (c) $H/L = 0.6$; (d) $H/L = 1.0$. Hard foundation (shale): (e) $H/L = 0.0$; (f) $H/L = 0.2$; (g) $H/L = 0.6$; (h) $H/L = 1.0$.

Fig. 7 presents the vibrational mode (2, 3) for the plate structure resting on the weak (clay) or hard foundations (shale) and for the depth ratios, $H/L = 0.0$, 0.2, 0.6 and 1.0. All the edges of the plate structure are considered as clamped. As can be seen from Fig. 7, the mode (2, 3) displays different vibrational patterns for each depth ratio. However, it can be observed from the same figure that the *in vacuo* vibrational forms are almost the same as the fully submerged case ($H/L = 1.0$). This is because the coupling between the *in vacuo* modes for the fully submerged case is very weak, and therefore, the modal forms remain nearly unchanged. It should also be noted that the frequencies of the plate structure increase with increasing hardness of the foundation and they decrease with increasing submerging depth.

Furthermore, the calculations were repeated for the plate clamped along its edges and resting on a medium hard foundation (sand and gravel). For these calculations, the depth ratio was taken as $H/L = 0.5$. In Fig. 8, the first eight *wet* vibrational modal forms are presented. It can be seen from the figure that the part of the plate in contact with water shows high levels of vibration. This is due to the inertial effect of the surrounding water.

4. Conclusions

A method of analysis is presented for investigating the effects of elastic foundation and fluid on the dynamic characteristics of elastic plate structures. A mixed-type finite element formulation was employed for the

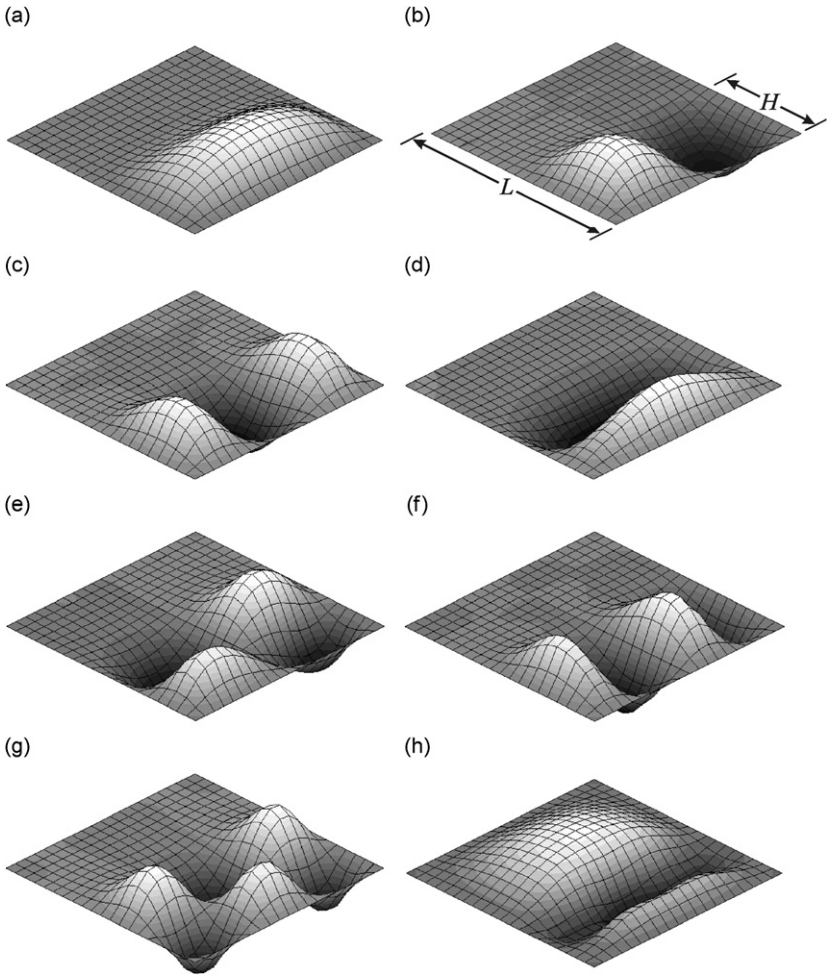

Fig. 8. Mode shapes of a plate structure resting on a medium hard foundation (sand and gravel) and clamped along its edges, for submerging depth ratio, $H/L = 0.5$: (a) first mode ($i = 1, j = 1$); (b) second mode ($i = 1, j = 2$); (c) third mode ($i = 1, j = 3$); (d) fourth mode ($i = 2, j = 1$); (e) fifth mode ($i = 2, j = 2$); (f) sixth mode ($i = 1, j = 4$); (g) seventh mode ($i = 2, j = 3$); (h) eight mode ($i = 3, j = 1$).

in vacuo analysis of the structure by using the Gâteaux differential for the derivation of the functional for the Kirchhoff plate–Pasternak-type elastic foundation interaction. For the calculation of the fluid–structure interaction effects a boundary integral equation method was adopted together with the method of images in order to impose an appropriate boundary condition on the fluid's free surface.

From the results given in this study, the calculations based on the presented method behave as expected. That is to say, the frequencies of the plate structure contacting an elastic foundation increase with increasing hardness of the foundation, and the *wet* frequencies of the foundation–plate–fluid system decrease with increasing area of contact with the fluid. The finite element and boundary element methods adopted in this study were verified before in the open literature (see, for instance, Refs. [5–7,15,22,23]).

As can be seen from Tables 7 and 8, the generalized added mass parameters are symmetric, and off-diagonal terms represent the effect of coupling between the *in vacuo* modes. It can also be concluded from Tables 7 and 8 that the coupling becomes stronger with decreasing submerging depth ratio.

The structural and fluid idealizations are independent and both depend on the complexity of the structure and the convergence of the results. To test the convergence of the finite element and boundary element methods, various numbers of finite elements and boundary elements were distributed over the plate structure. The *in vacuo* dynamic characteristics obtained using the mix finite element formulation were adopted for the

wet calculations. It can be realized from Tables 1–4 that the finite element and boundary element results converge with increasing number of elements and hydrodynamic panels, respectively.

It can be observed from Figs. 6–8 that the *wet* part of the plate structure shows high levels of vibration compared with the rest of the plate structure.

The present work has demonstrated the versatility of the method (finite element—boundary element method) developed for the analysis of the foundation–plate–fluid interaction systems.

Acknowledgment

This research was financially supported by the Scientific and Technological Research Council of Turkey (TUBITAK Project No. 105M041). This support is gratefully acknowledged.

References

[1] A.W. Leissa, *Vibration of Plates (NASA SP-160)*, Office of Technology Utilization, Washington, DC, 1969.
[2] J.N. Reddy, R.A. Arciniega, Shear deformation plate and shell theories: from Stavsky to present, *Mechanics of Advanced Materials and Structures* 11 (2004) 535–582.
[3] E. Winkler, *Die Lehre von der Elasticität und Festigkeit*, Prag, Dominicus, 1867.
[4] U.S. Gupta, A.H. Ansari, S. Sharma, Buckling and vibration of polar orthotropic circular plate resting on Winkler foundation, *Journal of Sound and Vibration* 297 (3–5) (2006) 457–476.
[5] M.H. Omurtag, A. Özütok, A.Y. Aköz, Y. Özçelikörs, Free vibration analysis of Kirchhoff plates resting on elastic foundation by mixed finite element formulation based on Gâteaux differential, *International Journal for Numerical Methods in Engineering* 40 (1997) 295–317.
[6] Y. Özçelikörs, M.H. Omurtag, H. Demir, Analysis of orthotropic plate–foundation interaction by mixed finite element formulation using Gâteaux differential, *Computers and Structures* 62 (1) (1997) 93–106.
[7] A.N. Doğruoğlu, M.H. Omurtag, Stability analysis of composite-plate foundation interaction by mixed FEM, *Journal of Engineering Mechanics, American Society of Civil Engineers* 126 (9) (2000) 928–936.
[8] D. Zhou, Y.K. Cheung, S.H. Lo, F.T.K. Au, Three-dimensional vibration analysis of rectangular thick plates on Pasternak foundation, *International Journal for Numerical Methods in Engineering* 59 (2004) 1313–1334.
[9] N. Eratlı, A.Y. Aköz, Free vibration analysis of Reissner plates by mixed finite element, *Structural Engineering and Mechanics* 13 (2002) 277–298.
[10] P.C. Dumir, Circular plates on Pasternak elastic foundations, *International Journal for Numerical and Analytical Methods in Geomechanics* 11 (1987) 51–60.
[11] H.S. Shen, J. Yang, L. Zhang, Free and forced vibration of Reissner–Mindlin plates with free edges resting on elastic foundations, *Journal of Sound and Vibration* 244 (2001) 299–320.
[12] Y. Xiang, C.M. Wang, S. Kitipornchai, Exact vibration solution for initially stressed Mindlin plates on Pasternak foundation, *International Journal of Mechanical Sciences* 36 (1994) 311–316.
[13] C.M. Wang, Y. Xiang, Q. Wang, Axistmmetric buckling of Reddy circular plates on Pasternak foundation, *Journal of Engineering Mechanics, American Society of Civil Engineers* 127 (2001) 254–259.
[14] L. Yu, H.-S. Shen, X.-P. Huo, Dynamic responses of Reissner–Mindlin plates with free edges resting on tensionless elastic foundations, *Journal of Sound and Vibration* (2007).
[15] A. Ergin, B. Uğurlu, Linear vibration analysis of cantilever plates partially submerged in fluid, *Journal of Fluids and Structures* 17 (2003) 927–939.
[16] Y. Fu, W.G. Price, Interactions between a partially or totally immersed vibrating cantilever plate and the surrounding fluid, *Journal of Sound and Vibration* 118 (1987) 495–513.
[17] K.-H. Jeong, G.-H. Yoo, S.-C. Lee, Hydroelastic vibration of two identical rectangular plates, *Journal of Sound and Vibration* 272 (2004) 539–555.
[18] T.-P. Chang, M.-F. Liu, On the natural frequency of a rectangular isotropic plate in contact with fluid, *Journal of Sound and Vibration* 236 (2000) 547–553.
[19] K.-H. Jeong, K.-J. Kim, Hydroelastic vibration of a circular plate submerged in a bounded compressible fluid, *Journal of Sound and Vibration* 283 (2005) 153–172.
[20] M.K. Kwak, S.B. Han, Effect of fluid depth on the hydroelastic vibration of free-edge circular plate, *Journal of Sound and Vibration* 230 (2000) 171–185.
[21] Y.K. Cheung, D. Zhou, Hydroelastic vibration of a circular container bottom plate using the Galerkin method, *Journal of Fluids and Structures* 16 (2002) 561–580.
[22] A. Ergin, P. Temarel, Free vibration of a partially liquid-filled and submerged, horizontal cylindrical shell, *Journal of Sound and Vibration* 254 (2002) 951–965.
[23] A. Ergin, B. Uğurlu, Hydroelastic analysis of fluid storage tanks by using a boundary integral equation method, *Journal of Sound and Vibration* 275 (2004) 489–513.

[24] J.T. Oden, J.N. Reddy, *Variational Methods in Theoretical Mechanics*, Springer, Berlin, Germany, 1976.
[25] P.L. Pasternak, On a new method of analysis of an elastic foundation by means of two foundation constants, Gosudarstvennoe Izdatelstvo Literaturi po Stroitelstvu i Arkhitekture, Moscow, Russia, 1954.
[26] A. Ergin, The response behavior of a submerged cylindrical shell using the doubly asymptotic approximation method (DAA), *Computers and Structures* 62 (1997) 1025–1034.
[27] L.C. Wrobel, *The Boundary Element Method, Applications in Thermo-Fluid and Acoustics*, Vol. 1, Wiley, New York, 2002.
[28] A. Ergin, W.G. Price, R. Randall, P. Temarel, Dynamic characteristics of a submerged, flexible cylinder vibrating in finite water depths, *Journal of Ship Research* 36 (1992) 154–167.